Supporting information for: High-mobility toolkit for quantum dot films

Francisco M. Gómez-Campos,[†,‡] Salvador Rodríguez-Bolívar,[†,‡] and Marco Califano [*,¶]

Departamento de Electrónica y Tecnología de Computadores, Facultad de Ciencias, Universidad de Granada, 18071 Granada, Spain , CITIC-UGR, C/ Periodista Rafael Gómez Montero, n 2, Granada, Spain , and Institute of Microwaves and Photonics, School of Electronic and Electrical Engineering, University of Leeds, Leeds LS2 9JT, United Kingdom

E-mail: m.califano@leeds.ac.uk

Atomistic modelling of single CQDs

In our atomistic approach the CQD is built with bulk-like structure, starting from its constituent atoms, from its center outwards up to the desired radius. This procedure yields surface atoms with unsaturated bonds. Atoms with only one (saturated) bond are removed, leaving on the surface only atoms with one or two missing bonds. These surface dangling bonds are passivated by pseudo-hydrogenic, short-range potentials with Gaussian form, positioned along the line connecting the missing bonding atom and the passivated atom, at a distance $0 < d < D_{\text{bulk}}$ (where D_{bulk} is the bulk bond length) from the

---
[*]To whom correspondence should be addressed
[†]Granada
[‡]CITIC-UGR
[¶]Leeds

center of the latter.[1,2] This method is not meant to simulate specific ligands, but represents rather a generic passivation that aims at removing states in the gap.

As it is the case with any non-self-consistent (i.e., non-DFT) method,[5] the structure is not relaxed nor the surface is allowed to reconstruct, since with realistic experimental sizes, this energy minimization step is prohibitively expensive computationally and cannot be performed self-consistently.

Tight-binding band structure parameters

When interband coupling is neglected, the effective mass at Γ (q=0) relative to miniband i of the 2D periodic system can be expressed within the tight-binding model as:[3]

$$m_i^*(q=0) = \frac{\hbar^2}{\alpha_i V_{ii} a^2} \tag{S1}$$

where $V_{ii} = \langle \psi_i(r)|V(r)|\psi_i(r-r')\rangle$ represents the coupling between neighboring states with angular momentum $i = s, p, d, \ldots$, $a = 2R + d$ is the center-to-center distance between nearest-neighbor CQDs (or, in other words, the lattice constant, or period, of the array), and α_i is a constant that depends on the specific lattice and state (i).[4]

In this framework, there is a direct relationship between coupling V_{ii} and corresponding miniband width W_i,[5]

$$W_{1i} = \gamma_i |V_{ii}| \tag{S2}$$

(where $\gamma_{1S} = 8$, $\gamma_{1P} = 4$ in both square and hexagonal lattices, and $V_{pp\pi}$ has been neglected). Using Eq. (S2), Eq. (S1) can be expressed as

$$m_i^*(q=0) = \frac{\beta_i \hbar^2}{W_i a^2} \tag{S3}$$

where β_i is a constant that depends on the specific lattice and state i. We find that this popular relationship is quite accurate, and even in the worst cases (i.e., for small sepa-

rations, when interband coupling is strongest and its applicability is questionable), this expression still yields effective masses that are within about 30% of one of the values we obtained by fitting the calculated band structure around q=0 with a parabola

$$m_i^* = \frac{\hbar^2 q_i^2}{2(E_i - E_0)} \tag{S4}$$

where $i = x, y$ are two perpendicular in-plane directions (see Table I), E_i is the calculated energy at $q = q_i$ (for q_i close to 0), and E_0 is the energy at $q = 0$.

Dependence of the band-structure parameters on the inter-dot separation
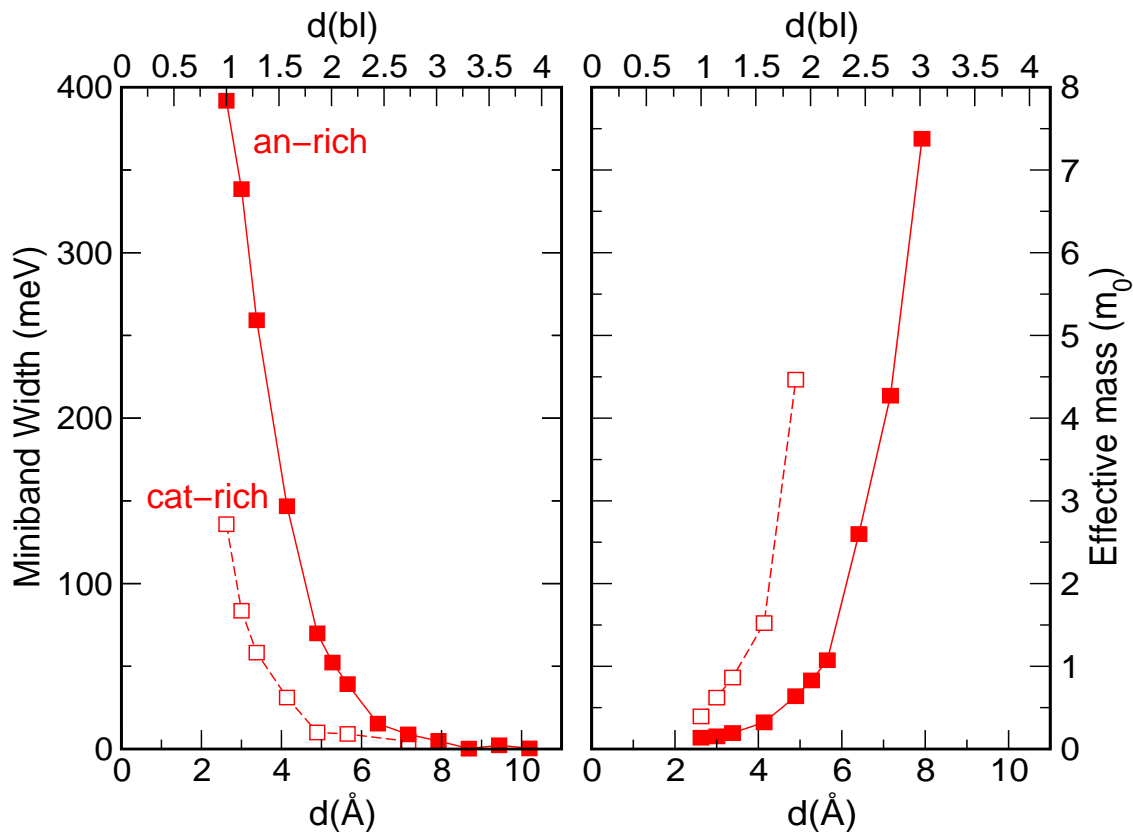
S 1: Miniband widths (a) and effective masses at Γ (b) calculated, as a function of inter-dot spacing expressed both in Å (bottom x axis), and in bond lengths (bl, top x axis), for the lowermost miniband in 2D arrays of InAs CQDs with $R = 1.22$ nm. Results relative to anion-rich and cation-rich surfaces are represented by solid symbols and lines and empty symbols and dashed lines, respectively.

Size-dependence of the band structure

The behavior of the parameters presented in Table I as a function of the dot size in the case of zinc-blende CdSe, is in agreement with the predictions of a general law for the effective band structure parameters, deduced for arrays of zinc-blende CdSe CQDs in a recent work:[5]

$$V_{ss} \approx A \left(\frac{5}{D} \right)^2 \left(\frac{c}{D} - 0.1 \right) \tag{S5}$$

where c is the diameter of a cylindrical section linking neighboring dots in the superlattice, $A = -26$ and D the dot diameter (We find that the choice $A = -22.3$ gives a better fit to our results).

The above expression therefore provides through Eq. (S2) an estimate for the miniband width in a 2D array of CQDs, that depends only on the dot size and the type of superlattice. Despite having been derived for $c/D > 0.1$, Eq. (S5) yields in our case ($c = 0$) an estimate for the 1S miniband (87 meV) in good agreement with our calculated value (76 meV).

We find however, that the values given above for the proportionality factor γ_i in Eq. (S2) are only valid in the *single-band approximation* i.e., when the coupling with higher bands is negligible. Whilst this treatment is appropriate at large inter-dot separations, it is not correct for very closely spaced dots, when the separation between s and p minibands is smaller than the miniband width. In this case the width W_{1i} is modified compared with the decoupled case: for *touching* (i.e., one bond length apart) InAs dots with $R = 1.2$ nm, the full miniband calculation (including 10 higher states) yields $W_{1S} = 392$ meV, (i.e., $\gamma_{1S} = 6.8$) compared with 463 meV, obtained using (S2) with $\gamma_{1S} = 8$ (i.e. considering the 1S state only). The factor 8 is recovered for distances larger than 0.5 nm (or 1.9 bl).

In the case of InAs arrays, instead, the calculated widths are only in *qualitative* agreement with the size dependence of Eq. (S5). We find that our InAs data are better repro-

duced by the following relationship

$$V_{ss}(\text{InAs}) \approx 2.126 \left(\frac{5}{D} \right)^{9/2}$$

which implies a much stronger size dependence than in Eq. (S5). Although the reduction in the overlap integral with increasing dot size is an effect common to all materials, result of the space normalization of the isolated-dot wave functions (i.e., the fact that, as the overall probability of finding the electron anywhere in the dot - given by the integral over the dot volume of the wave function squared - is 1, the probability of finding it at any specific location within the dot - given by the amplitude of the wave function at that location - decreases with increasing dot volume), the different size dependence we find in different materials does not simply reflect the general inverse-bulk-effective-mass scaling rule suggested in ref.[5]

In the case of wurtzite CdSe CQDs, we find the size dependence to be the same as that obtained for the zinc blende crystal structure, i.e., $V_{ss} = B(5/D)^2$, but with a slightly larger value for the proportionality constant ($B = 6$, compared with $A = 2.2$).

Effect of different surface morphologies
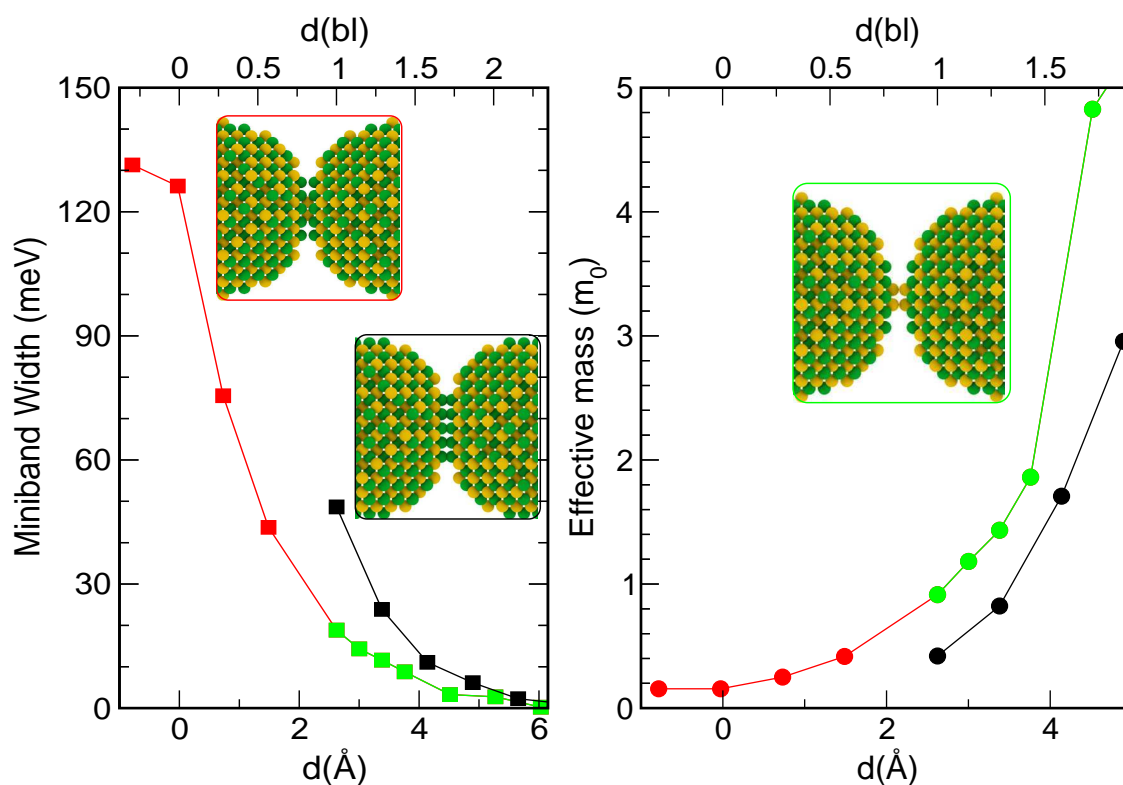
S 2: Miniband widths (a) and effective masses at Γ (b) calculated, as a function of inter-dot spacing expressed both in Å (bottom x axis), and in bond lengths (bl, top x axis), for the lowermost miniband in 2D arrays of InAs CQDs with $R = 2.0$ nm with surfaces terminated by (i) flat In atomic planes (black symbols and lines), (ii) a layer of two As atoms on top of the In atomic planes (blue symbols and lines), and (iii) two LEGO-like interlocking As atoms (red symbols and lines). Negative values for the dot-to-dot separation indicate that the surface outermost atom of one dot penetrates beyond the surface outermost atom of its neighbours. In this case (iii) however, the surface atoms of neighbouring dots do not overlap as they are rotated with respect to each other. Details of these three different interface morphologies are visualized in the insets, where yellow and green spheres represent As and In atoms, respectively.

An order-of-magnitude expression for the mobility

Assuming that the electrons are scattered by fluctuations in the dot size alone,[6] we derive the following expression for an order-of-magnitude estimate of the mobility in the lowest miniband of a CQD film[7]

$$\mu_{OM}(\rho_{\text{defects}}, \delta R) = \frac{e\hbar^3}{m^{*2}\rho_{\text{defects}}MA} \tag{S6}$$

where e is the electron charge, ρ_{defects} is the density of scattering centers (i.e., defect dots with radius $R - \delta R$),

$$M = \frac{1}{K_{q=0}^2}\left|\sum_h\sum_k b_h^* b_k \int \phi_h^*(\vec{r})\Delta V(\vec{r})\phi_k(\vec{r})d\vec{r}\right|^2 \tag{S7}$$

depends on the scattering potential (i.e., the difference ΔV between the potential of a CQD with radius R and one with radius $R - \delta R$),

$$K_q = \sum_h\sum_k b_h^* b_k \left\{\delta_{hk} + \sum_{R_p \neq 0} \exp^{i\vec{q}\cdot\vec{R}_p} \int \phi_h^*(\vec{r})\phi_k(\vec{r} - \vec{R}_p)d\vec{r}\right\}, \tag{S8}$$

ϕ_n are the single-dot wave functions, b_n are their tight-binding expansion coefficients, R_p is the position of the nearest neighbors, A is the unit cell area, and m^* is the effective mass of the miniband, obtained using Eq. (S4) (see columns 6, 7 and 8 in Table I).

References

(1) Wang, L.-W.; Zunger, A. Pseudopotential Calculations of Nanoscale CdSe Quantum Dots. *Phys. Rev. B* **1996**, *53*, 9579.

(2) Bester, G. Electronic Excitations in Nanostructures: An Empirical Pseudopotential Based Approach *J. Phys.: Condens. Matter* **2009**, *21*, 023202.

(3) Ashcroft, N. W.; Mermin, N. *Solid State Physics*, Holt Rinehart and Winston, New York, London, 1976.

(4) $\alpha_{1S} = 2$ for the 1S state in 2D and 3D square lattices, $\alpha_{1S} = 3$ for the same state in a 2D hexagonal lattice,[3] $\alpha_{1S} = 4$ for the 1S state in a close packed 3D hexagonal lattice, $\alpha_{Ns1S} = 3Ns$ for Ns degenerate 1S states in a 2D hexagonal lattice ($Ns = 4$ for PbSe), $\alpha_{1Px,y} = 1$ for the 1Px and 1Py states in a 2D square lattice, $\alpha_{1P} = 2/3$ for the 1P states in a 3D square lattice, …

(5) Delerue, C. From Semiconductor Nanocrystals to Artificial Solids with Dimensionality Below Two. *Phys. Chem. Chem. Phys.* **2014**, *16*, 25734-25740.

(6) Shabaev, A; Efros, Al. L; Efros, A. L. Dark and Photo-Conductivity in Ordered Array of Nanocrystals. *Nano Lett.* **2013**, *13*, 5454-5461.

(7) Gómez-Campos, F. M.; Rodríguez-Bolívar, S.; Califano, M. Effective Approach for an Order-of-Magnitude-Accurate Evaluation of the Electron Mobility in Colloidal Quantum Dot Films. (unpublished)